



Molecular Crystals and Liquid Crystals Science and Technology. Section A. Molecular Crystals and Liquid Crystals

Publication details, including instructions for authors and subscription information:

<http://www.tandfonline.com/loi/gmcl19>

Excitons in the Surface of Aromatic Hydrocarbon Crystals Studied by Biphotonic Electron Emission

Masaki Ono^{a b} & Masahiro Kotani^a

^a Faculty of Science, Gakushuin University, Mejiro, Tokyo, 171-8588, Japan

^b Institute for Molecular Science, Okazaki, 444-8585, Japan

Version of record first published: 24 Sep 2006

To cite this article: Masaki Ono & Masahiro Kotani (2001): Excitons in the Surface of Aromatic Hydrocarbon Crystals Studied by Biphotonic Electron Emission, Molecular Crystals and Liquid Crystals Science and Technology. Section A. Molecular Crystals and Liquid Crystals, 355:1, 85-103

To link to this article: <http://dx.doi.org/10.1080/10587250108023656>

PLEASE SCROLL DOWN FOR ARTICLE

Full terms and conditions of use: <http://www.tandfonline.com/page/terms-and-conditions>

This article may be used for research, teaching, and private study purposes. Any substantial or systematic reproduction, redistribution, reselling, loan, sub-licensing, systematic supply, or distribution in any form to anyone is expressly forbidden.

The publisher does not give any warranty express or implied or make any representation that the contents will be complete or accurate or up to date. The accuracy of any instructions, formulae, and drug doses should be independently verified with primary sources. The publisher shall not be liable for any loss, actions, claims, proceedings, demand, or costs or damages whatsoever or howsoever caused arising directly or indirectly in connection with or arising out of the use of this material.

Excitons in the Surface of Aromatic Hydrocarbon Crystals Studied by Biphotonic Electron Emission

MASAKI ONO* and MASAHIRO KOTANI

Faculty of Science, Gakushuin University, Mejiro, Tokyo, 171-8588, Japan

(Received December 15, 1999; In final form February 12, 2000)

The dynamics of excitons in the surface region has been studied with five aromatic hydrocarbon crystals, anthracene, pyrene, fluoranthene, coronene, and α -perylene through electron emission which occurs through excitonic processes. Fusion (annihilation) and photoionization of excitons have been found to be the major processes which lead to the emission, although there are indications of the participation of other less important processes. Factors determining the dominant process under a specific condition are discussed. The lifetimes of the excitons in the surface region of crystals of anthracene, pyrene and fluoranthene are found to be the same as those in the bulk, while shorter lifetimes have been found in crystals of coronene and α -perylene. Quenching by adsorbed oxygen is proposed as the origin of the difference in the behaviours.

Keywords: Photoemission; Aromatic hydrocarbon crystal; Exciton; photoionization

1. INTRODUCTION

Multiphoton ionization is a powerful technique for the investigation of excited states. This technique has been applied to various phases; atoms, molecules, clusters, and surface of metals and semiconductors. In the case of two-photon ionization, electrons are emitted by resonant direct two-photon ionization (R2PI), or photoionization of excited states.

In organic crystals electrons are often emitted by another process. In aromatic hydrocarbon crystals an electronic excited state can migrate as an exciton. When the excitons collide with each other, an exciton can ionize while the other exciton relaxes to the ground state. This is called exciton fusion, or exciton-exciton annihilation. The exciton fusion is accordingly a quadratic effect. In order to distin-

* Present address: Institute for Molecular Science, Okazaki, 444-8585, Japan

guish ionization via exciton fusion with standard ionization through two-photon absorption, we use in this paper the term “biphotonic ionization” after M. Pope, who first found the biphotonic emission of electrons from an anthracene crystal [1]. Pott and Williams [2] and Haarer and Castro [3] measured the excitation spectrum of biphotonic electron emission from anthracene crystals, and discussed the mechanisms. Katoh et al. showed that electrons were emitted from an anthracene crystal through fusion of two singlet excitons [4]. Our group has observed in α -perylene [5], pyrene [6] and fluoranthene [7] electron emission that exhibits, on pulsed excitation, a long tail, demonstrating unambiguously that exciton fusion leads to electron emission in these crystals.

However, exciton fusion is not the only mechanism for biphotonic emission. Photoionization of an exciton can also occur. There are several reports on photoionization of excited states in organic crystals [8]. Photoemission of conduction electrons, generated by another light has been observed in β -carotene [9]. Later, photoionization of triplet state of Zn-phthalocyanine [10] has been measured by ultraviolet photoelectron spectroscopy with additional visible light irradiation.

Until now considerable effort has been made to clarify different mechanisms operating in different materials. It has not been systematically investigated, however, what determines the processes which dominates under a specific condition. In this article we study the mechanism for five typical aromatic hydrocarbon crystals, pyrene, anthracene, fluoranthene, coronene and α -perylene, and discuss the factors which determine the dominating process.

The escape depth of an electron excited by an UV photon is only a few nanometers, or a few molecular layers, although the penetration depth of light is much larger. Accordingly, photoemission bears information of a very thin surface region. It is possible, by studying the photoemission of excitonic origin, to gain knowledge concerning the behaviour of the excitons in the surface region. The latter may be sensitive to adsorbed gases, and also to the molecular arrangement, which can be different from that in the bulk.

2. METHODS AND EXPERIMENTAL

2.1 Sample preparation

Single crystals of fluoranthene, α -perylene, anthracene and pyrene were grown by the Bridgman method from extensively zone-refined materials. Pyrene was pre-purified by Diels-Alder reaction with maleic anhydride. A platelet of single crystal, cut from an ingot, was pasted on a stainless steel plate with silver paste. The typical size of the sample was $5 \times 5 \times 0.5 \text{ mm}^3$ for electron emission meas-

urements. Coronene, obtained from Ardlich, was purified by vacuum sublimation. Electron emission from coronene was studied with a sub-micron thick film prepared on a stainless steel substrate by vacuum sublimation. All samples, including evaporated films, were exposed to the air before they were transferred to the vacuum chamber for measurement. Fluorescence lifetimes were determined with single-photon counting using a nitrogen nanosecond lamp, constructed in the laboratory. The electronics was the same as in the time-correlated single-electron counting.

2.2 Time-correlated single-electron counting

The time profile of the electron emission excited by a pulsed light gives information on the temporal distribution of the emission events. If electron emission occurs by photoionization of exciton, electrons are emitted only during the light pulse. If, on the other hand, exciton fusion is responsible, electron emission continues as long as the excitons survive. In this way, the time profile indicates clearly the mechanism. The decay constant should be equal to a half of the exciton lifetime, since the rate of a bimolecular reaction decays twice as fast as compared to the density of the reactant.

The system for time-correlated single-electron counting has been described in Ref. [5]. A dye laser, pumped by a XeCl excimer laser, or the 3rd or 4th harmonics of Q-switched Nd: YAG laser was used as the light source. For measurements of short lifetimes a quenched transient dye laser (QTDL, 1 ns FWHM) was constructed [11]. The excitation pulse was divided into two. One excited the sample. The other was detected by a fast pin photodiode (Hamamatsu, S-1188) and provided the start signal for a time-to-amplitude converter (TAC, CAMBERRA 1443A) via a discriminator (CAMBERRA 1433). Electrons emitted from the crystal were amplified by a microchannel plate (MCP, Hamamatsu F2221-21S) and the signal was fed to the TAC as the stop signal through an amplifier (LeCROY, 133B) and a discriminator. The intensity of the exciting light was kept very low ($\sim 10 \mu\text{J}/\text{cm}^2$ shot), in order to avoid electrical charging of the sample specimen. The sample was held at a high negative potential (-1 kV), so that the flight time of the electrons was insensitive to the initial kinetic energy. Care was taken to limit the irradiated area to the sample surface so that electron emission from sample holder or other parts of the vacuum system does not interfere.

2.3 TOF measurements

The electronics was the same as in the time-correlated single-electron counting. The light was incident at the sample surface at 30 degrees. The electrons drifted

to the detector (MCP) in a field-free region. The length of the drift space was 67 mm.

2.4 Autocorrelation method

This type of measurements were performed by using a double pulse excitation. The amount of electrons emitted depends on the interval between the pulses. When the interval, Δt , is infinitely large, the total amount of electrons is twice as large as that generated by a single pulse. In contrast, the total amount is four times as large as that by a single pulse at $\Delta t = 0$, since biphotonic electron emission is a quadratic phenomenon. The relationship between the amount of the electrons and Δt is determined by the temporal shape of the excitation pulses and the lifetime of the intermediate state. Hence, the lifetime of the intermediate state can be obtained from its analysis when the pulse shape is known.

The rate equation for the exciton density, $[S^*]$, is given by

$$\frac{d[S^*]}{dt} = \alpha I(t) - \frac{1}{\tau}[S^*] - \gamma_{SS}[S^*] \quad (1)$$

where α , $I(t)$, τ_{S^*} , and γ_{SS} are the absorption coefficient at the excitation wavelength, the intensity of the excitation light, the lifetime of the exciton and the rate constant of bimolecular annihilation, respectively. The excitation pulses are assumed to be a Gaussian. The pulse width is 10 ns. We neglect the term proportional to the square of the exciton density in eq. (1), since in the present experiment the intensity of the exciting light was kept so low that bimolecular annihilation was not important.

The amount of electrons emitted is calculated by

$$N(\Delta t) \propto \int_{-\infty}^{\infty} [S^*]^2 dt \quad (2)$$

for exciton fusion and by

$$N(\Delta t) \propto \int_{-\infty}^{\infty} [S^*]^2 I(t) dt \quad (3)$$

for photoionization of exciton. The traces of N vs. Δt are almost the same in both cases. Accordingly, the lifetime can be obtained without specifying the mechanism, whether exciton fusion or photoionization of excitons. Hence the measurement of autocorrelation can be a powerful tool for assigning an intermediate state.

The arrangement for autocorrelation measurements has been described in Ref. [11]. Excitation was made with a Q-switched Nd:YAG laser and a dye laser, pumped by a XeCl excimer laser. The pulse widths of the lasers were both 10 ns.

A digital delay generator (Stanford Research, DG 535) provided trigger pulses, suitably delayed, for both lasers, and also for a Boxcar integrator. The jitter of the pulse-to-pulse interval was 10 ns. Electrons emitted were amplified with a micro-channel plate whose output was processed with a Boxcar integrator (Stanford Research, SR250).

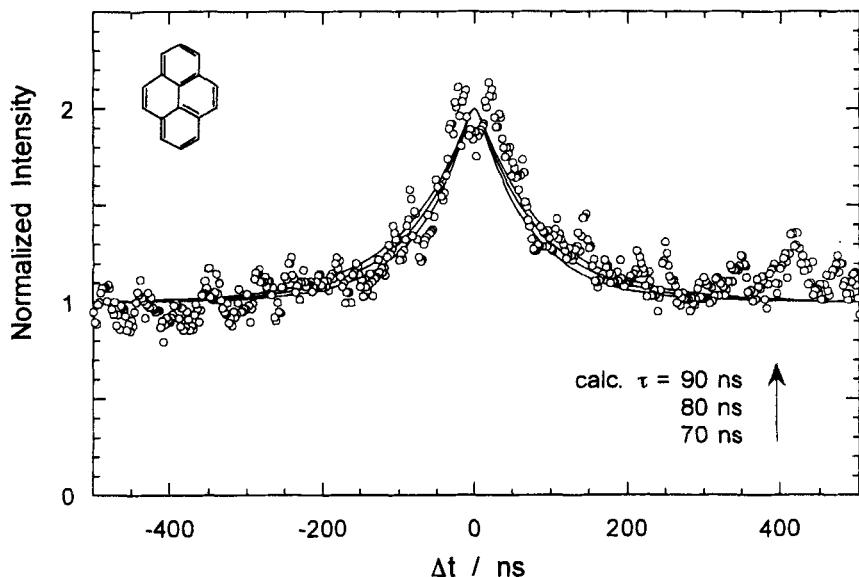


FIGURE 1 Autocorrelation trace of electron emission from a pyrene single crystal. Excitation is made at 355 nm. The solid curves are theoretical fit. The result indicates that the intermediate state involved has a lifetime of 80 ± 10 ns

3. RESULTS

3.1 Pyrene

The amount of electrons emitted from a pyrene single crystal is proportional to the square of the intensity of the incident light [6]. This indicates that electron emission occurs by a biphotonic process. Excitation is made at 270 nm and at 355 nm. The photon energies, when doubled, exceed the ionization potential of the material (5.58 eV [13]).

The time profile of the biphotonic electron emission from a pyrene single crystal, measured with the time-correlated single-electron counting, shows an exponential decay for all excitation wavelengths [6]. The emission has a tail, a

phenomenon which indicates that it occurs by exciton fusion. The exciton lifetime should be twice as long as the decay time observed, 35 ~ 48 ns, i.e. 70 ~ 96 ns. This coincides fairly well with the fluorescence lifetime measured with the same specimen of the pyrene crystal, 100 ns. This indicates that the fusion of excimer excitons is the mechanism and that the lifetime of the excimer exciton at the surface is equal to that in the bulk.

Figure 1 shows the results of an autocorrelation measurement. The excitation was made at 355 nm. The abscissa is the interval between the two excitation pulses, and the ordinate is the total amount of electrons emitted, normalized to the sum of the electrons emitted by two independent pulses. At $\Delta t = 0$ ns the normalized intensity is 2. This is exactly the value predicted from the quadratic dependence on light intensity and indicates that the measurement has been made properly. The curves are the theoretical fits. Judging from the fit, the lifetime of the intermediate state involved is 80 ± 10 ns. This lifetime indicates that the excimer excitons are involved in the biphotonic electron emission.

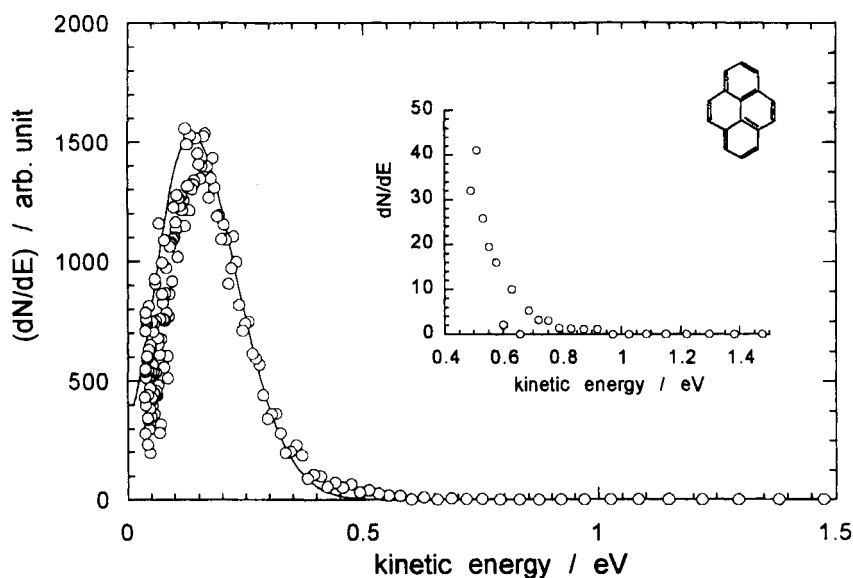


FIGURE 2 A time-of-flight spectrum of electrons emitted from a pyrene crystal. Excitation at 355 nm. The inset shows the expanded view of the higher energy region. The maximum kinetic energy of the emitted electrons is 0.8 eV

Figure 2 shows the kinetic energy distribution, measured by the TOF. The open circles are experimental points, obtained with 355 nm excitation. As we know

already, the emission is delayed. This has been convoluted with the time-of-flight and the results are shown in solid lines in the Figure. The distribution has a peak at 0.15 eV. However, the most important feature of the result may be the maximum energy and not the position of the peak. This is clear if one considers the efficient energy loss process an electron experiences in the escape from the solid. The maximum energy observed is ~ 0.8 eV (see the inset in Fig. 2). The maximum kinetic energy expected from exciton fusion is calculated with the known energy of the excimer exciton (3.16 eV) and the ionization potential of a pyrene crystal (5.58 eV): $2 \times 3.16 \text{ eV} - 5.58 \text{ eV} = 0.74 \text{ eV}$ and is consistent with time-resolved measurements.

All of the results indicate that biphotonic emission of electrons in a pyrene crystal occurs through the fusion (annihilation) of the excimer excitons. There is no indication that the lifetime of the exciton in the surface region differs from that in the bulk.

3.2 Anthracene

The number electrons emitted is proportional to the square of the excitation intensity when the excitation is made at 355 nm and the intensity was kept low. At higher intensities the dependence changes into a linear one, indicating that exciton fusion becomes important at high exciton densities [4].

The time profile of the electron emission from an anthracene single crystal shows an exponential decay with time constant of 5 ns [6]. Considering that the emission is quadratically dependent on the excitation, this indicates the exciton lifetime of 10 ns.

Figure 3 shows the results of autocorrelation measurements of an anthracene single crystal. The excitation is made again at 355 nm. The lifetime of the intermediate state involved is obtained to be 10 ± 5 ns, the same result as obtained by the time-correlated single-electron counting.

A longer fluorescence lifetime is observed when a fairly thick crystal is measured. Depending on the size of the crystal and also on the temperature of the measurement, the apparent fluorescence lifetime varies from 10 ns to 20 ns. This is due to the reabsorption of the fluorescence. When extrapolated to a thickness of zero, the results of the measurements converge to 10 ns.

Figure 4 shows the kinetic energy distribution of electrons emitted by 355 nm excitation. This maximum energy observed, 0.5 eV, coincides with the kinetic energy, expected from the exciton fusion model; $2 \times 3.11 \text{ eV} - 5.67 \text{ eV} = 0.55 \text{ eV}$.

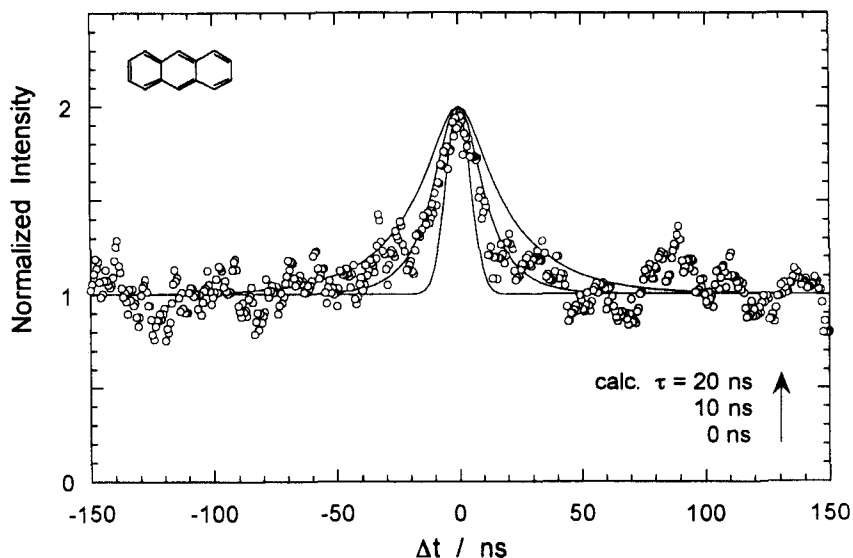


FIGURE 3 Autocorrelation trace of electron emission from an anthracene single crystal. Excitation is made at 355 nm. The solid curves are theoretical fit. The result indicates that the intermediate state involved has a lifetime of 10 ns

In summarizing, biphotonic electron emission occurs in anthracene by the fusion of singlet excitons. The observed lifetime at the surface, 10 ns, coincides with that in the bulk.

3.3 Fluoranthene

The light intensity dependence of the electron emission is quadratic, when excitation is made at 410 nm, 340 nm, and 266 nm, indicating a biphotonic mechanism [7]. The ionization potential has been reported to be 6.14 eV [14]. With excitation at 410 nm and at 415 nm, electrons are still emitted by some biphotonic process, although the total two-photon energy is less than the ionization potential. The reason for this puzzle is not clear. It is possible that the reported ionization potential is too high.

The time profile of electron emission, measured with time-correlated single-electron counting has been discussed in Ref. [7]. Different time profiles are obtained for different excitation wavelengths (Fig. 5). When excited at 415 nm, electrons are emitted during the pulse irradiation only. When the wavelength becomes shorter (410 nm, 360 nm and 330 nm), the time profile starts to exhibit

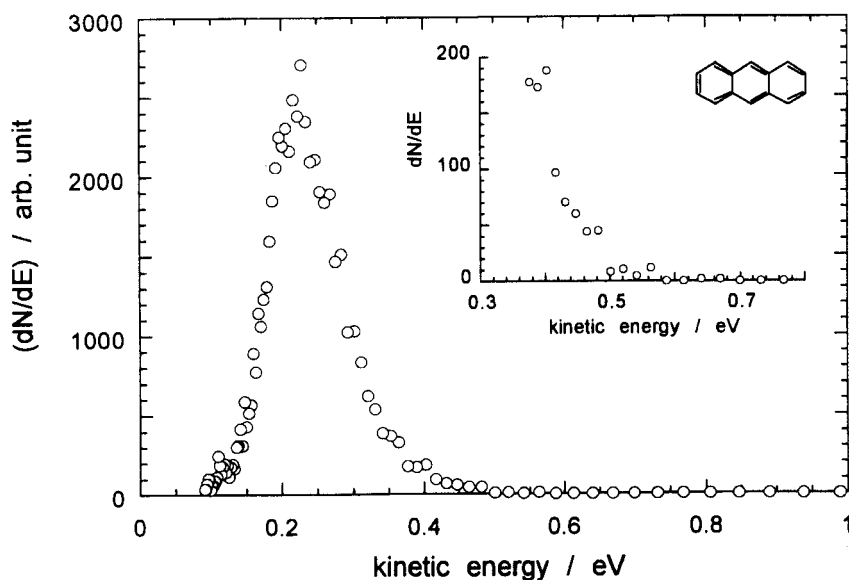


FIGURE 4 A time-of-flight spectrum of electrons emitted from an anthracene crystal. Excitation at 355 nm. The maximum kinetic energy of the emitted electrons is 0.5 eV

a decay. With excitation at even shorter wavelengths (325 nm and 266 nm), the electron emission becomes impulsive again.

With 415 nm excitation, which corresponds to the absorption edge, only singlet excitons are created. The impulsive emission indicates that electrons are emitted by photoionization of some excited state, possibly trapped electrons.

With 410 nm excitation, delayed emission is observed. Its decay constant (47 ns) coincides with the fluorescence lifetime (48 ns). This indicates that the ionization occurs not by the fusion of two singlet excitons, but by the collision of a singlet exciton with a state having a much longer lifetime, such as a trapped electron. Ionization through the collision of a singlet and a triplet exciton may be excluded since the total energy gained by the fusion, $2.95 \text{ eV} + 2.35 \text{ eV}$ [15] = 5.30 eV, is smaller than the ionization potential of the crystal.

As the excitation wavelength becomes shorter, the decay time changed to 25 ns, corresponding to one half of the fluorescence lifetime of the crystal, 48 ns. This is interpreted as indicating the exciton fusion.

Above 3.81 eV (325 nm) the emission turns to be instantaneous again. Considering that the excitation is being made with a 10 ns pulse, two possibilities exist for the mechanism in this energy range. One is that the fusion of an intermediate

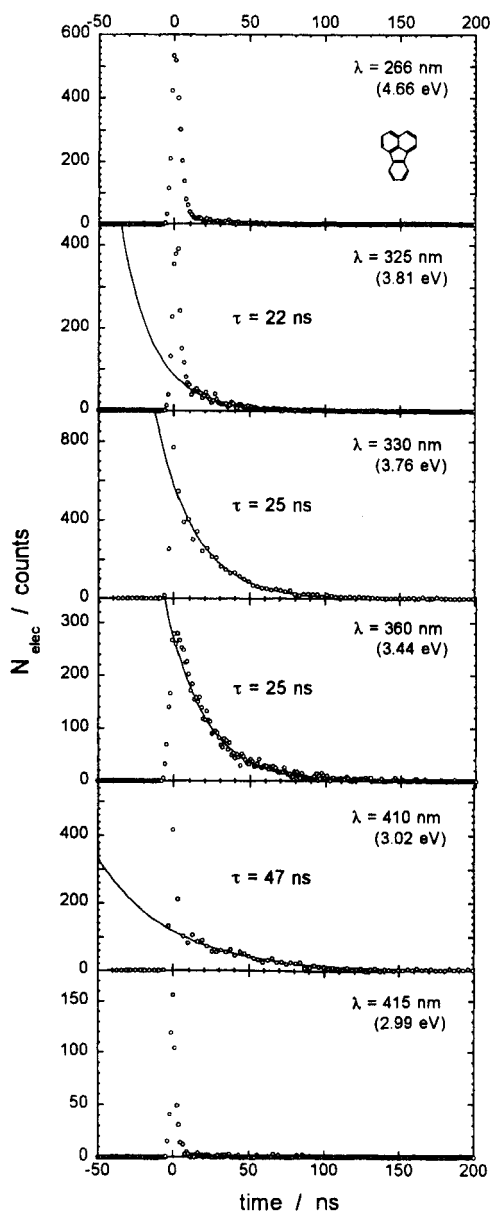


FIGURE 5 Results of time-correlated single-electron counting measurements of electron emission from a fluoranthene single crystal (Reproduced from Ref. [7]). It is seen that the mechanism of electron emission changes as the excitation energy is varied. Photoionization, which gives rise to an instantaneous emission, and fusion of excitons, which leads to a delayed emission, coexist at some excitation energies

state is occurring, which has a lifetime much shorter than the laser pulse. The second possibility is the photoionization of an intermediate state, that can have any lifetime. Autocorrelation measurements give the answer.

The results of autocorrelation measurements indicate that the intermediate state involved is 50 ± 10 ns for both 355 nm and 266 nm excitations [7]. This lifetime coincides with that of the singlet excitons, a fact that indicates that the electron emission induced by the excitation in this energy range is due to photoionization of the exciton..

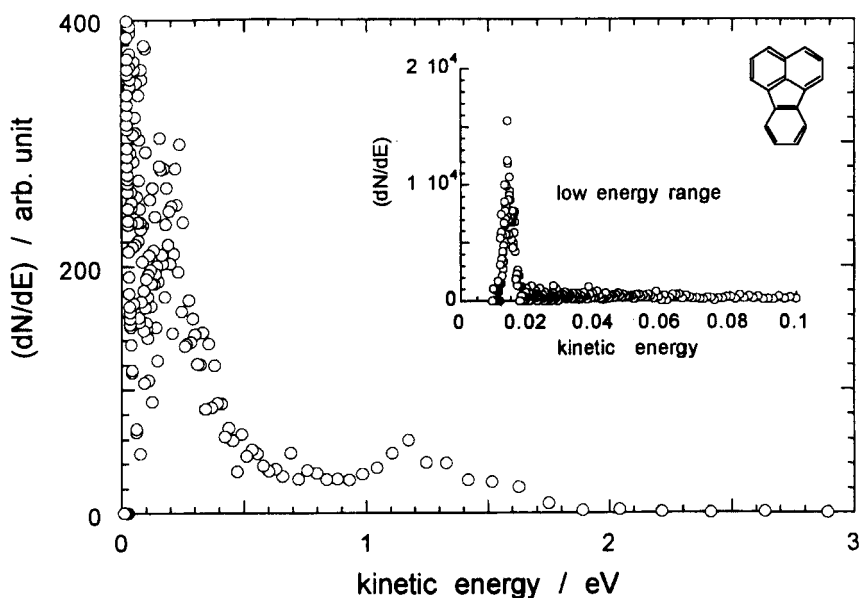


FIGURE 6 A time-of-flight spectrum of electrons emitted from a fluoranthene crystal. Excitation at 355 nm. The large peak around 0.02 eV is ascribed to electrons emitted by exciton fusion, while the peak at 0.2 eV is considered to be due to photoionization of excitons. The origin of the prominent peak around 1.2 eV is tentatively assigned to a three-photon process

Figure 6 shows the kinetic energy distribution of electrons, excited at 355 nm. A large peak is observed at a low energy, and in the higher energy region there are two peaks.

We assign the large peak at 0.02 eV to the signal due to electrons emitted by the fusion of singlet excitons which is the main process at 355 nm excitation. The kinetic energy expected from the fusion mechanism is $2 \times 2.95 \text{ eV} - 6.14 \text{ eV} = -0.24 \text{ eV}$, which implies that no electron can be emitted by this process. It is possible that the ionization potential reported of this material is not correct. If this is

the case, the ionization potential should be $2 \times 2.95 \text{ eV} - 0.02 \text{ eV} = 5.88 \text{ eV}$. Assuming that this ionization potential is correct, the kinetic energy of electrons, which is expected, is calculated for various processes. The kinetic energy is 0.56 eV for photoionization of the exciton, and 1.10 eV for direct (nonresonant) two-photon ionization. The peak at 0.2 eV has been assigned to photoionization of singlet exciton. The origin of electrons extending to 1.8 eV is not clear. A kinetic energy of more than 1.1 eV is not possible by biphotonic processes, and hence these electrons could be due to a three-photon process.

The mechanism of biphotonic electron emission from a fluoranthene single crystal changes with photon energies. In the absorption edge and above 3.81 eV (325 nm) electrons are emitted mainly through photoionization of an exciton. In the intermediate range, where absorption is strong, exciton fusion is dominant. No difference has been found between the lifetime at the surface and in the bulk. In the absorption edge region emission involving some long-lived trapped states is observed, the nature of which is unknown.

3.4 Coronene

The ionization potential of a coronene crystal has been reported to be 5.30 eV [16]. When the excitation is made at 355 nm, which can generate S_2 excitons, a quadratic dependence is observed of the emission (Fig. 2 of Ref. [12]). Results of an autocorrelation measurement of a coronene film indicate that the lifetime of the intermediate state is 15 ns. An additional long-lived intermediate with a much longer lifetime is present which can be a triplet exciton (we have verified through a measurement of delayed fluorescence that the triplet lifetime is 25 ms in the coronene crystal). Photoionization of triplet exciton (2.37 eV[17] + 3.49 eV) is, at least on energy grounds, possible, but the energy obtained by a triplet-triplet annihilation ($2 \times 2.37 \text{ eV}$) is not sufficient for ionization.

The fluorescence lifetime of a coronene film is 25 ns. There is a small ($\sim 1\%$) contribution from a component with a lifetime of 110 ns. It is assigned to an excimer [12]. The shorter lifetime component is tentatively assigned to a free singlet exciton, although the lifetime appears to be too long for a free exciton (in a pyrene crystal the lifetime of a free exciton is reported to be 10 ps [18]). The lifetime obtained from the electron emission is shorter than the fluorescence lifetime.

The results of the single-electron counting measurements are shown in Figure 7. The QTDL pulses of 1 ns pulse width, is used for excitation. Most of the electrons are emitted instantaneously, indicating photoionization. The excited states photoionized may include triplet excitons and free singlet excitons. A small contribution of delayed emission with a decay constant of $\sim 7 \text{ ns}$ can be

recognized in the Figure. When doubled, this decay time corresponds to the lifetime, 15 ns, obtained in the autocorrelation measurement, indicating the fusion of singlet excitons.

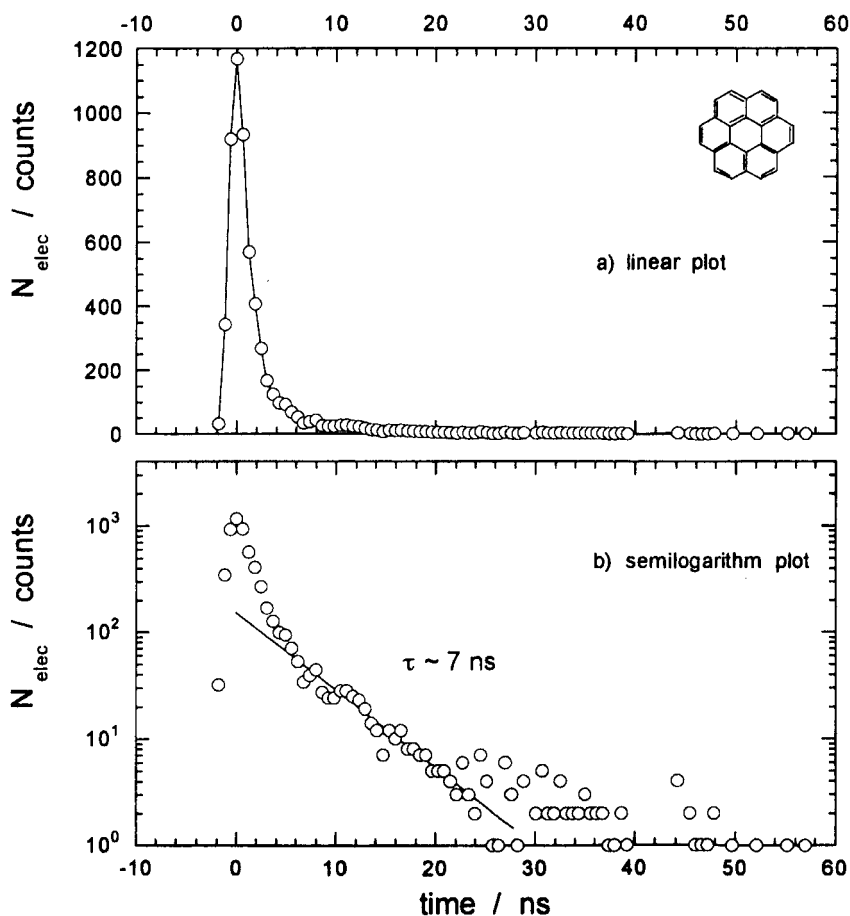


FIGURE 7 Results of time-correlated single-electron counting measurements of electron emission from an evaporated film of coronene. Emission is instantaneous, but a small contribution of delayed emission which decays with 7 ns lifetime, is also present. This decay is consistent with the fusion of singlet excitons whose lifetime is 15 ns

The kinetic energy distribution of the emitted electrons is shown in Figure 8. Two peaks are found, one at 0.5 eV and another at 0.15 eV. The maximum energy is about 1.0 eV, which corresponds to the energy expected for photoionization of a free exciton, $2.88 \text{ eV} + 3.49 \text{ eV} - 5.30 \text{ eV} = 1.07 \text{ eV}$. This supports the results

of time-resolved measurements. The peak near 0.15 eV could be a vibrational structure of a cation. However, it is also possible that another intermediate is responsible which has a different ionization potential, a triplet exciton, for example.

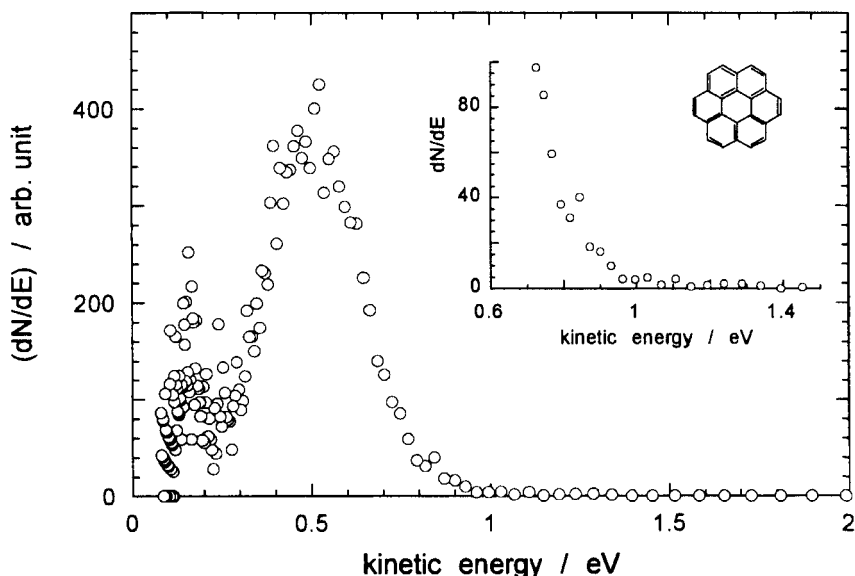


FIGURE 8 A time-of-flight spectrum of electrons emitted from an evaporated film of coronene. Excitation at 355 nm. The maximum kinetic energy of the emitted electrons is 1.0 eV, which is interpreted as due to photoionization of free exciton

In a coronene crystal the main process is the photoionization of an excited state with a lifetime of 15 ns, which is shorter than the lifetime of a singlet exciton in the bulk (25 ns). Photoionization of triplet exciton, and also fusion of the singlet excitons, make a small contribution.

3.5 α -Perylene

The lifetime of the intermediate state involved has been determined to be 15 ns from autocorrelation measurements [12]. This coincides with the lifetime, 15 ns, of the excimer exciton at the surface, measured by single electron counting [5]. However, this lifetime is shorter by a factor of four than the lifetime of the excimer in the bulk (65 ns), obtained from fluorescence lifetime measurements.

The response becomes prompt when the excitation is made at shorter wavelengths [5]. Obviously the mechanism changes from exciton fusion to photoionization as the excitation energy increases.

Figure 9 shows the kinetic energy distribution of emitted electrons. Excitation is made at 355 nm. A peak at 0.25 eV is assigned to the photoionization of excimer exciton. The maximum kinetic energy in the photoionization of an excimer exciton is estimated to be 0.89 eV, using the energy of the exciton, the photon energy, and the ionization potential. The maximum kinetic energy observed is 1.4 ± 0.1 eV. The difference of 0.5 eV is beyond the error in the estimation and may indicate the existence of a minor process by which electrons with a higher energy can be generated. One possibility is the photoionization of conduction electrons, suggested by Katoh and Kotani [5]. The band gap for α -perylene has been reported to be 3.1 eV [19], and the maximum kinetic energy of this process is expected to be 1.47 eV.

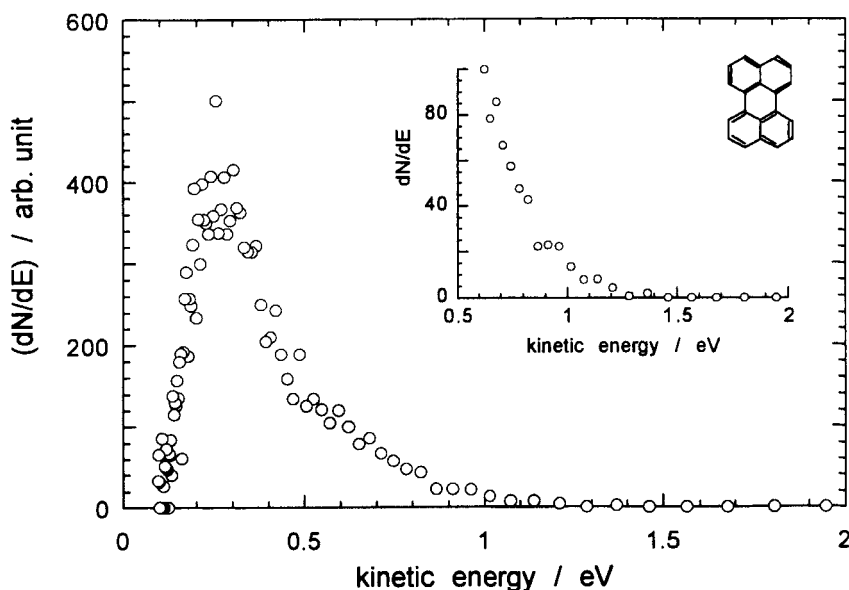


FIGURE 9 A time-of-flight spectrum of electrons emitted from a single crystal of α -perylene. Excitation at 355 nm. The maximum kinetic energy expected from photoionization of the excimer excitons is 0.89 eV. The maximum energy observed is 1.4 eV and is tentatively assigned to photoemission of electrons from the conduction band

In α -perylene crystal photoionization of excimer exciton is the dominant process with 355 nm excitation. Photoionization of some higher-lying excited state, possibly of conduction electrons, coexists. At longer wavelengths, 460 nm for example, electrons are emitted by the fusion of the excimer excitons. Thus the main mechanism changes, as in the case of a fluoranthene crystal, according as

the excitation energy. The lifetime of the excimer exciton at the surface region (15 ns) is shorter than that in the bulk (65 ns).

4. DISCUSSION

4.1 Efficiency of biphotonic electron emission

The mechanism of biphotonic electron emission can be different depending on the material and excitation energy. Two main processes are (1) photoionization and (2) fusion (annihilation) of singlet excitons. Which mechanism is dominant depends on the excitation condition and the compound. Direct, unresonant two-photon ionization may be ignored when the excitation is resonant to a real intermediate state, since a nonresonant excitation has a much smaller cross section compared to resonant processes.

The amount of electrons emitted, N , is given in eq. (4) for the fusion of singlet excitons,

$$N_{SS} \propto \gamma_{SS} \Phi_{AI} [S^*]^2 V \quad (4)$$

and eq. (5) for photoionization of S^* ,

$$N_{PI} \propto \sigma_{S^*}(\lambda) I [S^*] V \quad (5)$$

where Φ_{AI} is the autoionization yield for a highly excited state generated by exciton fusion, V is the volume responsible for the electron emission, $\sigma_{S^*}(\lambda)$ is the photoionization cross section of the singlet exciton and I is the incident light intensity. Using a steady state approximation, $[S^*]$ is substituted for $\alpha I \tau_{S^*}$.

$$N_{SS} = \gamma_{SS} \Phi_{AI} \alpha(\lambda)^2 \tau_{S^*}^2 \cdot I^2 V \quad (6)$$

$$N_{PI} = \sigma_{S^*}(\lambda) \alpha(\lambda) \tau_{S^*} \cdot I^2 V \quad (7)$$

We define the yields, Φ_{SS} and Φ_{PI} , by

$$\Phi_{SS} = \gamma_{SS} \Phi_{AI} \alpha(\lambda)^2 \tau_{S^*}^2 \quad (8)$$

$$\Phi_{PI} = \sigma_{S^*}(\lambda) \cdot \alpha(\lambda) \tau_{S^*} \quad (9)$$

The relative yields is given by

$$\frac{\Phi_{SS}}{\Phi_{PI}} = \frac{\gamma_{SS} \Phi_{AI} \alpha(\lambda) \tau_{S^*}}{\sigma_{S^*}(\lambda)} \quad (10)$$

In the case of fluoranthene the dominant process changes as the photon energy is varied. This is a clear indication that both processes, exciton annihilation and

photoionization of the excitons, can be of comparable efficiency. Actually, according to our experience the former is more often encountered.

An important parameter is the mobility of the exciton. Excitons must move efficiently and collide with each other in order for annihilation to occur. The bimolecular rate constant γ_{SS} is expressed by $4\pi DR$ in solution, where D is the diffusion coefficient and R is the reaction radius. This may apply qualitatively also for exciton fusion in a crystal. The bimolecular rate constant vary widely from compound to compound: $\gamma_{SS} = 10^{-8} \sim 10^{-15} \text{ cm}^3\text{s}^{-1}$ [20]. Anthracene exhibits a large γ_{SS} , while it is small in a crystal of fluoranthene ($1.8 \times 10^{-11} \text{ cm}^3\text{s}^{-1}$ [21]) and α -perylene ($8 \times 10^{-14} \text{ cm}^3\text{s}^{-1}$ [22]).

In the case of a compound which has a large γ_{SS} , Φ_{SS} is larger than Φ_{PI} in the entire energy region. The photoionization of exciton can be the dominant process only in a compound which has a small γ_{SS} . Another important parameter is the absorption coefficient. A large absorption coefficient means a small penetration depth of the exciting light and hence an exciting light with a large absorption coefficient gives rise to a large concentration of the exciton in a thin layer close to the surface. In a fluoranthene crystal photoionization of the singlet exciton is observed with excitation in the absorption edge and above 3.81 eV, while in the intermediate region electrons are emitted by exciton fusion. In an α -perylene a similar behaviour is observed: exciton fusion dominates at 460 nm and photoionization of exciton at 355 nm [5].

4.2 The lifetime of an exciton in the surface region

Lifetimes of the exciton at the surface region have been obtained with five aromatic hydrocarbon crystals. In pyrene, anthracene and fluoranthene the lifetime observed in the electron emission coincides with the fluorescence lifetime. In crystals of coronene and α -perylene they are shorter than those in the bulk. In the case of anthracene the spectral overlap between the absorption and the fluorescence is large, and the fluorescence lifetime is lengthened by reabsorption. When a due care is taken in the measurements, the fluorescence lifetime agrees with the lifetime deduced from the electron emission. Luminescence spectra of coronene and α -perylene are of excimer character, i.e. broad and red-shifted, and the overlap is small. Nevertheless the lifetimes at the surface are short. This indicates that some other factors should be considered.

Singlet exciton can be efficiently quenched by energy transfer to oxygen, which may be adsorbed on the surface. Crystals of small organic compounds have often a high vapour pressure and new surface always appears by constant evaporation. But the speed of this self-cleaning depends on the vapor pressure. Accordingly, oxygen may remain on the surface if the vapor pressure is low. In

fact compounds whose lifetime at the surface is short, coronene and α -perylene, have low vapor pressures. Compounds with higher vapor pressures, anthracene, pyrene and fluoranthene, exhibit the same lifetimes irrespective of whether on the surface or in the bulk.

The lifetime can also be affected by the arrangement of molecules. If the surface structure is different from that in the crystal, the lifetime can also be different. In a sandwich arrangement such as found in α -perylene crystal, the singlet excitons relax into the excimer exciton. The radiative relaxation into the ground state of such a sandwich-type excimer is forbidden, and, as a result, the lifetime of an excimer is long. It is often assumed that the surface reconstruction is not important in molecular crystals, considering the small intermolecular interaction. However, structures only present in the surface may not be a rare phenomenon, if we think about the frequent occurrence of many crystal modifications of organic crystals and phase transformations between them. These different crystal phases are thermodynamically very close to each other in energy.

5. CONCLUSION

We have determined the mechanism of biphotonic emission of electrons for five aromatic hydrocarbon crystals. Three types of measurements have been combined: single electron counting and autocorrelation method, both for determining the lifetime of the intermediate excited state involved, and time-of-flight measurements for determining the kinetic energy of the emitted electrons. Interplay of exciton fusion and photoionization of the exciton in determining the dominant mechanism under a specific condition has been critically examined. It is concluded that exciton fusion dominates in most cases. Photoionization of excitons are only found in systems in which excitons are not very mobile, and hence the exciton fusion is inefficient. Exciton lifetimes shorter than those in the bulk, observed in coronene and α -perylene crystals, are suggested to be due to quenching by adsorbed oxygen.

Acknowledgements

This paper has been dedicated to the lasting memories of our beloved friend, Edgar Silinsh.

We wish to thank Professor K. Seki for stimulating comments. We are indebted to Dr. R. Katoh for advice and helpful discussion, and also for a gift of purified anthracene and pyrene. Messers. H. Miyagi and Y. Shimokawa of the machine shop of Gakushuin University contributed through their skilful work

and advice in the construction of the instruments. Purification and crystal growth of α -perylene crystals were made by Mr. S. Takahashi. Ms. M. Tanaka kindly made the data of γ_{SS} of fluoranthene available to the authors prior to publication. MO acknowledges the Research Fellowships of the Japan Society for the Promotion of Science (JSPS) for Young Scientists.

References

1. M. Pope, H. Kallmann, and J. Giachino, *J. Chem. Phys.* **42** (1965) 2540.
2. G.T. Pott and D.F. Williams, *J. Chem. Phys.* **51** (1969) 203.
3. D. Haarer and G. Castro, *Chem. Phys. Letters* **12** (1971) 277.
4. R. Katoh, M. Ogiu, and M. Kotani, *Chem. Phys. Letters* **174** (1990) 531.
5. R. Katoh and M. Kotani, *Chem. Phys. Letters* **196** (1992) 103.
6. M. Ono, R. Katoh and M. Kotani, *Proc. SPIE* **2362** (1995) 219.
7. M. Ono and M. Kotani, *Chem. Phys. Letters* **295** (1998) 493.
8. R. Katoh and M. Kotani, *Chem. Phys. Letters* **174** (1990) 537.
9. M. Wautelet, L.D. Laude and A.H. Madjid, *Chem. Phys. Letters* **51** (1977) 530.
10. E.E. Koch, *Phys. Scripta* **T17** (1987) 120.
11. F.R. Schaefer, L. Wenchong and S. Szatmari, *Appl. Phys.* **B 32** (1983) 123.
12. M. Ono and M. Kotani, *Chem. Phys. Letters* **295** (1998) 34.
13. N. Sato, H. Inokuchi, B.M. Schmid and N. Karl, *J. Chem. Phys.* **83** (1985) 5413.
14. *Landolt-Boernstein Numerical Data and Fundamental Relationship in Science and Technology* (Springer, Berlin, 1985), New Series, **III 17 1**, 154.
15. S.L. Morov, *Handbook of Photochemistry* (Merzel Dekker, New York, 1973). T_1 energy in nonpolar solvent.
16. K. Seki, T. Hirooka, Y. Kamura and H. Inokuchi, *Bull. Chem. Soc. Jpn.* **49** (1976) 904.
17. K. Ohno and H. Inokuchi, *Chem. Phys. Letters* **23** (1973) 561.
18. B. Walker, H. Port and H.C. Wolf, *Chem. Phys.* **92** (1985) 177.
19. N. Sato, K. Seki and H. Inokuchi, *J. Chem. Soc. Faraday Trans.* **II 77** (1981) 1621.
20. A. Braun, U. Meyer, H. Auweter, H.C. Wolf and D. Schmidt, *Z. Naturforsch.* **37a** (1982) 1013.
21. M. Tanaka and M. Kotani, to be published.
22. A. Inoue, K. Yoshihara and S. Nagakura, *Bull. Chem. Soc. Jpn.* **45** (1972) 1973.